BER Sensitivity to Mistiming in Ultra-Wideband Impulse Radios—Part I: Nonrandom Channels

Zhi Tian, *Member, IEEE,* and Georgios B. Giannakis, *Fellow, IEEE*

***Abstract*—We investigate timing tolerances of ultra wideband (UWB) impulse radios. We quantify the bit-error-rate (BER) sensitivity to epoch timing offset under different operating conditions, including frequency flat fading channels, dense multipath fading channels, multiple access with time hopping, and various receiver types including sliding correlators and RAKE combiners. Our systematic approach to BER derivations under mistiming can be extended to a wide range of channel fading types. Through analyses and simulations, we illustrate that the reception quality of a UWB impulse radio is highly sensitive to both timing acquisition and tracking errors. In particular, time-hopping-based multiple-access systems exhibit little tolerance to acquisition errors, and the energy capture capability of a RAKE combiner can be severely compromised by mistiming.**

***Index Terms*—Mistiming, performance analysis, RAKE receiver, synchronization, ultra wideband communications.**

I. Introduction

ULTRA WIDEBAND (UWB) impulse radios (IRs) convey information symbols using a stream of impulse-like carrierless pulses of very low power density and ultra-short duration: typically a few tens of picoseconds to a few nanoseconds. The ultra wide bandwidth exposes signals to fine time resolution and offers potential for ample multipath diversity. It has been demonstrated that the fading margin required to compensate for dense multipath is much lower than what is needed for narrowband communications [1]. These properties position UWB as a favorable candidate for short-range indoor high-speed wireless communications [2] and for outdoor *ad hoc* networking with low probability of detection and capability to overlay existing wireless systems [3].

The unique advantages of UWB IR technology are somewhat encumbered by stringent timing requirements because the transmitted pulses are very narrow and have low power. Accurate timing imposes major challenges to UWB systems in realizing their potential bit error rate (BER) performance, capacity, throughput, and network flexibility. It has been shown through simulations that system throughput degrades markedly for relatively modest increase in timing jitter and even diminishes when the pulse-level tracking error is only a tenth of the pulse duration [4]. However, neither multipath nor is the impact of symbol-level acquisition errors is considered in [4].

The operating conditions of UWB systems vary in different applications. Outdoor propagation is typically dominated by a direct path, whereas indoor settings entail dense multipath propagation [5]. Time hopping (TH) is typically employed to enable multiple access and smooth the transmit spectrum [2]. In a rich-multipath environment, the system performance heavily relies on the receiver structure, which ranges from a simple sliding correlator to various types of RAKE combiners. The diverse mechanisms of direct path versus dense multipath propagation, with and without TH, as well as the various receiver options, lead to different implications of the timing acquisition and tracking errors. This paper addresses the timing tolerances of UWB IR transmissions for a broad range of operation settings. Sensitivity to mistiming is investigated by quantifying the BER degradation due to both acquisition and tracking errors. Both pulse amplitude modulation (PAM) and pulse position modulation (PPM) are considered. Such analyses shed light on the implications of mistiming to UWB impulse radio design and guide the design of allowable margins for timing offset estimation in UWB system development.

In our BER sensitivity analysis, we adopt a two-step procedure that is often carried out for performance analysis over fading channels. First, the BER is expressed as a $Q(\cdot)$ function that depends on the given realization of the random channel parameters. This instantaneous performance is then integrated over the joint probability density function (pdf) of the random parameters to obtain the average BER. The overall analysis is presented in a two-part sequel. Here, Part I outlines our system model and operating transceiver conditions in the ensuing Section II. For PAM transmissions under various operating conditions, Section III analyzes the BER degradation induced by mistiming for fixed channel realizations, with illustrative figures shedding light on the implications of mistiming in different propagating environments. Part II will focus on BER analysis in fading channels [6]. The energy capture capability of RAKE receivers under mistiming will be quantified in a unified manner. Results for PPM will also be summarized in [6], along with extensive corroborating simulations. Motivated by current UWB implementations, we focus on binary modulation and confine our discussions to binary PAM/PPM throughput this sequel.

Manuscript received April 23, 2003; revised February 27, 2004. Z. Tian was supported by the National Science Foundation under Grant CCR-0238174. G. B. Ginnakis was supported by the Army Research Laboratory/CTA under Grant DAAD19-01-2-011 and the National Science Foundation under Grant EIA-0324804. Parts of the work in this paper were presented at the IEEE SPAWC Conference, Rome, Italy, June 2003 and the IEEE GLOBECOM Conference, San Francisco, CA, Dec. 2003. The associate editor coordinating the review of this manuscript and approving it for publication was Dr. Martin Haardt.

Z. Tian is with the Electrical and Computer Engineering Department, Michigan Technological University, Houghton, MI 49931 USA (e-mail: ztian@mtu.edu).

G. B. Giannakis is with the Electrical and Computer Engineering Department, University of Minnesota, Minneapolis, MN 55455 USA (e-mail: georgios@ece.umn.edu).

Digital Object Identifier 10.1109/TSP.2005.843747

II. Modeling

A UWB pulse $p(t)$ has ultra-short duration T_p at the (sub-)nanosecond scale, and its maximum permissible average transmit power is in the order of 0.5 mW, according to the Federal Communications Commission (FCC) mask [7]. In IR, every symbol is transmitted using N_f pulses $p(t)$ over N_f frames (one pulse per frame of frame duration $T_f \gg T_p$), which is equivalent to sending each symbol through a transmit filter $p_s(t) = \sum_{i=0}^{N_f-1} p(t - iT_f)$ of symbol duration $T_s := N_f T_f$. For multiple access, the user of interest suppresses multiple access interference (MAI) using a pseudo-random TH code sequence $c(i) \in [0, N_c - 1]$, which time-shifts each pulse position at multiples of the chip duration T_c, with $N_c T_c \leq T_f$ [2]. A system choosing a larger value for N_c typically allows for a larger user capacity. These codes hop on a frame-by-frame basis, but the hopping pattern remains invariant from symbol to symbol,[1] i.e., $c(i) = c(i + lN_f)$, $\forall l$, and $i \in [0, N_f - 1]$. The transmit filter with TH is given by $p_s(t) = \sum_{i=0}^{N_f-1} p(t - iT_f - c(i)T_c)$, which is scaled to have unit energy by setting $\int p^2(t)dt = 1/N_f$. With information-bearing binary PAM symbols $s(k) \in \{\pm 1\}$ being independent identically distributed (i.i.d.) with zero mean and average transmit energy per symbol $\mathcal{E}_s$, the transmitted pulse stream is [8]:

$$u(t) = \sqrt{\mathcal{E}_s} \sum_{k=0}^{\infty} s(k) p_s(t - kN_f T_f). \tag{1}$$

After propagating through a multipath channel, the received signal takes on the general form

$$\begin{aligned} r(t) &= \sum_{l=0}^{L} \alpha_l u(t - \tau_l) + v(t) \\ &= \sqrt{\mathcal{E}_s} \sum_{l=0}^{L} \alpha_l \sum_{k=0}^{\infty} s(k) \\ &\quad \times \sum_{i=0}^{N_f-1} p\left(t - kN_f T_f - iT_f - c(i)T_c - \tau_l\right) + v(t), \end{aligned} \tag{2}$$

where $(L + 1)$ is the total number of propagation paths, each with gain α_l being real-valued with phase shift 0 or π and delay τ_l satisfying $\tau_l < \tau_{l+1}$, $\forall l$. The channel is random and quasi-static, with $\{\alpha_l\}_{l=0}^{L}$ and $\{\tau_l\}_{l=0}^{L}$ remaining invariant within one symbol period but possibly changing independently from symbol to symbol. The additive noise term $v(t)$ consists of both ambient noise and MAI and is independent of $s(k)$, $\{\alpha_l\}_{l=0}^{L}$, and $\{\tau_l\}_{l=0}^{L}$. We focus on performance evaluation of the desired user, treating the composite noise $v(t)$ as a white Gaussian random process with zero-mean and power spectral density of $\mathcal{N}_o/2$. This assumption is widely used in performance analysis of communication systems and is justified at least for low SNR values, low data rates, or large spreading factors $N_f N_c$ [9].

[1]Other hopping patterns may also be used, such as long-code hopping, in which the TH codes repeat after several symbols, or slow hopping, in which the TH codes hop on a symbol-by-symbol basis but remain invariant for all frames within a symbol. The results derived in this paper can be easily generalized to other TH patterns.

Two special cases of fading channels arise: When $L = 0$, the channel is frequency flat, as considered in outdoor UWB ranging systems [10]. Indoor propagation channels, on the other hand, are typically characterized by dense multipath, i.e., $L \gg 0$ and $\tau_{l+1} - \tau_l < 2T_p$, $\forall l$; see, e.g., [11]–[14]. To isolate the channel delay spread, we define relative path delays $\tau_{l,0} := \tau_l - \tau_0$ for $l \in [0, L]$; the maximum delay spread is thus $\tau_{L,0} + T_p$. We select $T_f \geq \tau_{L,0} + 2T_p$ and set either $c(N_f - 1) = 0$ or $c(N_f - 1) \leq c(0)$ to avoid inter-symbol interference (ISI) when perfect timing can be acquired. With these definitions, the composite channel formed by convolving the physical channel with the pulse is given by $h(t) := \sum_{l=0}^{L} \alpha_l p(t - \tau_{l,0})$, and the equivalent received symbol-waveform of duration T_s can be expressed as $h_s(t) := \sum_{j=0}^{N_f-1} h(t - jT_f - c_j T_c) = \sum_{l=0}^{L} \alpha_l p_s(t - \tau_{l,0})$, which simplifies $r(t)$ to

$$r(t) = \sqrt{\mathcal{E}_s} \sum_{k=0}^{\infty} s(k) h_s(t - kT_s - \tau_0) + v(t). \tag{3}$$

A correlation-based receiver correlates $r(t)$ with a locally generated pulse train $p_s(t)$, time-shifted by a nominal propagation delay $\hat{\tau}$, to produce the sufficient statistic for symbol detection:

$$y(n) = \int_{nT_s + \hat{\tau}}^{(n+1)T_s + \hat{\tau}} r(t) p_s(t - nT_s - \hat{\tau}) dt. \tag{4}$$

Let us denote the timing mismatch as $\tau := \tau_0 - \hat{\tau} = N_\epsilon T_f + \epsilon$, where $N_\epsilon \in [0, N_f - 1]$, and $\epsilon \in [-T_p, T_f - T_p)$. The parameters $N_\epsilon T_f$ and ϵ indicate the breakdown of mistiming into *acquisition* and *tracking* errors, respectively; see Fig. 1 for graphical illustration of the timing information in both the frequency flat case and the dense multipath case. Notice that N_ϵ is limited to N_f finite values since timing is resolvable only within a symbol duration.

While this correlation receiver is suitable for AWGN and flat-fading channels, channels inducing frequency selective fading call for the use of RAKE receivers to collect the ample multipath diversity. As indicated by (3), the maximum energy capture under perfect timing can be achieved by using $h_s(t)$ as the receive-template for optimum matched filtering, which requires knowledge of the multipath channel. To investigate how mistiming may compromise the capability of RAKE reception in energy capture, we adopt a generic RAKE receiver structure with $(L' + 1)$ fingers, as shown in Fig. 2. The RAKE tap delays $\{\tilde{\tau}_{l',0}\}_{l'=0}^{L'}$ are design parameters that could be, but are not necessarily, chosen among the channel path delays $\{\tau_{l,0}\}_{l=0}^{L}$. In fact, we are motivated not to set $L' = L$ and $\tilde{\tau}_{l,0} = \tau_{l,0}$ in a dense multipath because a large number of RAKE fingers L' could lead to computationally prohibitive RAKE combining, not to mention the difficulty in estimating accurately both $\{\alpha_l\}_{l=0}^{L}$ and $\{\tau_{l,0}\}_{l=0}^{L}$. Alternatively, we may resort to a RAKE structure with equally spaced taps, i.e., $\tilde{\tau}_{l',0} := l' T_r$, with tap spacing $T_r \geq T_p$, and a maximum tap delay $\tilde{\tau}_{L',0} \leq T_f - 2T_p$. A full RAKE arises when $L' = L$, and each $\tilde{\tau}_{l',0}$ is matched to one of the delayed paths, whereas $L' < L$ corresponds to a "partial RAKE," which may be less effective in energy capture but computationally more affordable. In particular, the sliding correlator can be considered to be a "RAKE-1"

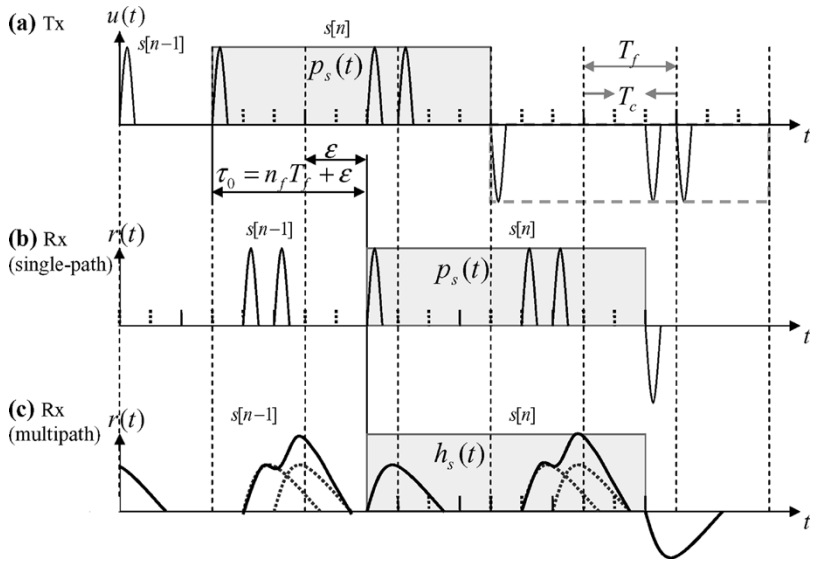

Fig. 1. Timing offsets in UWB impulse radios: $N_f = 3$, $T_c = T_f/3$, and the TH code sequence is [0,2,0]. (a) Transmitted waveform. (b) Received waveform in the single-path case. (c) Received waveform in the multipath case. Vertical dashed lines are frame boundaries with reference to the receiver's clock ($\hat{\tau} = 0$ and $\tau = \tau_0$). In this example, the symbol-level acquisition error is $(N_\epsilon = 1)T_f$, whereas the pulse-level tracking error is $\epsilon = 2T_c + T_p \in [-T_p, T_f - T_p)$.

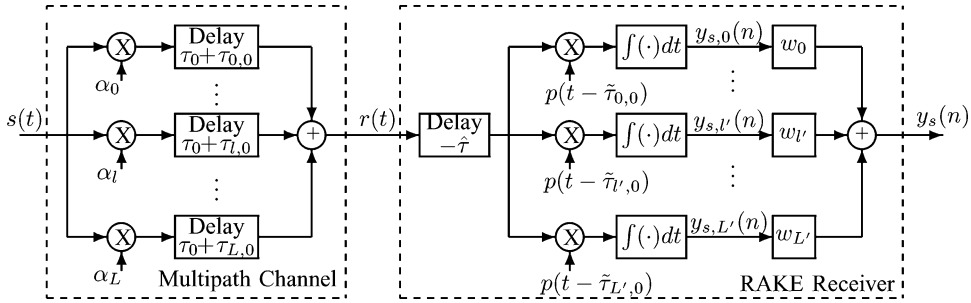

Fig. 2. Correlation-based receiver.

receiver with $L' + 1 = 1$ [14]. The RAKE weights $w_{l'}$ can be selected to represent maximum ratio combining, equal-gain combining, or other linear combining techniques. For all these combiners, the correlation template $p_s(t)$ in (4) is replaced by $p_s^{(rc)}(t) = \sum_{l'=0}^{L'} w_{l'} p_s(t - \tilde{\tau}_{l',0})$.

Both the sliding correlator and the RAKE receiver rely on the correlation between the transmit filter and the receiver template. Therefore, symbol detection hinges on the properties of the normalized auto-correlation function of $p(t)$, which are defined as $R_p(\tau) := N_f \int_{-\infty}^{\infty} p(t)p(t-\tau)dt \in [-1, 1]$. With these definitions, we combine (2) and (4) to reach a unifying expression for the detection statistic:

$$\begin{aligned} y(n) &= \int_{nT_s+\hat{\tau}}^{(n+1)T_s+\hat{\tau}} r(t) p_s^{(rc)}(t - nT_s - \hat{\tau})dt \\ &= \int_0^{N_f T_f} r(t + nN_f T_f + \hat{\tau}) \sum_{l'=0}^{L'} w_{l'} p_s(t - \tilde{\tau}_{l',0})dt \\ &= \sqrt{\mathcal{E}_s} \sum_{k=0}^{\infty} s(k) \sum_{i=0}^{N_f-1} \sum_{j=0}^{N_f-1} \sum_{l=0}^{L} \sum_{l'=0}^{L'} w_{l'} \alpha_l \frac{R_p(\Lambda_p)}{N_f} \\ &\quad + v(n) \end{aligned} \tag{5}$$

where $\Lambda_p := (k-n)N_f T_f + (i-j)T_f + (c(i)-c(j))T_c + N_\epsilon T_f + \epsilon + \tau_{l,0} - \tilde{\tau}_{l',0}$. For convenience, let $y_s(n) := y(n) - v(n)$ represent the noise-free (signal) component of the decision statistic. When the RAKE taps are normalized by $\sum_{l'=0}^{L'} w_{l'}^2 = 1$, the noise term $v(n)$ is Gaussian with zero mean and variance $\sigma_v^2 = (\mathcal{N}_o/2)$. It is worth stressing that (5) subsumes various operating conditions in terms of channel types, TH codes, and receiver structures, of which the interesting scenarios are listed in Table I. Stringent timing requirements come from the fact that $R_p(\tau)$ has a very narrow nonzero support. In (5), the values for k, i, and j contribute nonzero summands to $y(n)$ only when there exist l and l' such that the corresponding Λ_p falls in the range of $(-T_p, T_p)$, for given N_ϵ and ϵ. We will henceforth term such triplets (k, i, j) *nontrivial*.

III. Conditional BER Sensitivity for PAM

In this section, we investigate the impact of incorrect timing $(\tau = \tau_0 - \hat{\tau} \neq 0)$ on the symbol detection performance, conditioned on fixed channel realizations $\{\alpha_l\}_{l=0}^{L}$ and $\{\tau_l\}_{l=0}^{L}$. We will start with a UWB transmission over a simple AWGN channel, demodulated with a sliding correlator receiver. A single-user system (no TH) and a multiple-access system (with TH) will be discussed separately to illustrate the distinct impact of TH on the BER sensitivity. We will then proceed to the

TABLE I
VARIOUS TYPES OF OPERATING CONDITIONS

Parameters	Channel type	Receiver type	MA
$L=0, L'=0, \{c(i)\}_{i=0}^{N_f-1}=0$	frequency flat	correlator	no
$L=0, L'=0, \{c(i)\}_{i=0}^{N_f-1}\neq 0$	frequency flat	correlator	yes
$L\gg 1, L'=0$	dense multipath	correlator	yes/no[1]
$L\gg 1, 1\ll L'\leq L$	dense multipath	RAKE	yes/no[1]

[1] Both cases of multiple access are subsumed, depending on whether TH codes are employed.

dense-multipath case; both correlation-based and RAKE-based receivers will be studied to compare their capability in energy capture and robustness to mistiming. Throughout our analysis, we suppose that the receiver is able to achieve correct TH code synchronization after timing acquisition and tracking.

A. TH-Free PAM Transmissions Over AWGN Channels

When a TH-free UWB PAM signal propagates through a direct-path AWGN channel, we substitute $L=0$, $L'=0$, and $c(i)=0, \forall i$, in (5), which simplifies the detection statistic to

$$y_s(n)=\sqrt{\mathcal{E}_s}\sum_{k=0}^{\infty}s(k)\sum_{i=0}^{N_f-1}\sum_{j=0}^{N_f-1}\frac{w_0\alpha_0 R_p(\Lambda_p)}{N_f} \tag{6}$$

where $\Lambda_p=(k-n)N_fT_f+(i-j)T_f+N_\epsilon T_f+\epsilon$. Note that some of the terms in Λ_p are multiples of $T_f\gg T_p$. To identify nontrivial triplets (k,i,j) that satisfy $\Lambda_p\in(-T_p,T_p)$, it is instrumental to isolate those frame-level terms from the pulse-level terms. To this end, we introduce an integer q, which is set such that the frame-level portion of Λ_p is zero, and the pulse-level portion of Λ_p falls in $(-T_p,T_p)$:

$$\begin{aligned}&\text{(I. Frame level)}\quad (k-n)N_fT_f+(i-j)T_f+N_\epsilon T_f\\ &\qquad\qquad +qT_f=0;\\ &\text{(II. Pulse level)}\quad \epsilon-qT_f\in(-T_p,T_p).\end{aligned} \tag{7}$$

Condition (7.II) determines the allowable values for q and ϵ, while (7.I) describes the constraint on the triplet (k,i,j) to yield an admissible q. Since $\epsilon\in[-T_p,T_f-T_p)$, it is evident from (7.II) that the only possible value for q is $q=0$, which in turn confines the allowable range for ϵ to be $(-T_p,T_p)$. Meanwhile, since i, j, and $N_\epsilon\in[0,N_f-1]$, the nontrivial values for k can be deduced from (7.I) to be $(k-n)N_f=-(i-j)-N_\epsilon-q\in[-2(N_f-1),(N_f-1)]$, which leads to $(k-n)\in\{0,-1\}$. For each possible value of k, the associated i and j are further constrained such that $i=j-N_\epsilon-q-(k-n)N_f$ falls in $[0,N_f-1]$. When $j\in[N_\epsilon+q,N_f-1]$, the constraint $i<N_f$ excludes $k-n=-1$; hence, $k=n$ and $i=j-N_\epsilon-q$. Similarly, $j\in[0,N_\epsilon+q-1]$ leads to $k=n-1$, and $i=j-N_\epsilon-q+N_f$. With these constraints on q and (k,i,j), it follows from (7) that $\Lambda_p=\epsilon$, and the received signal in (6) is simplified to

$$\begin{aligned}y_s(n)&=w_0\alpha_0\sqrt{\mathcal{E}_s}\left(\sum_{j=N_\epsilon}^{N_f-1}s(n)\frac{R_p(\epsilon)}{N_f}+\sum_{j=0}^{N_\epsilon-1}s(n-1)\frac{R_p(\epsilon)}{N_f}\right)\\ &=w_0\alpha_0\sqrt{\mathcal{E}_s}R_p(\epsilon)\left(\left(1-\frac{N_\epsilon}{N_f}\right)s(n)+\frac{N_\epsilon}{N_f}s(n-1)\right).\end{aligned} \tag{8}$$

To evaluate BER performance in the presence of timing errors, we look at $y_s(n)$ conditioned on $(s(n),s(n-1))$. Note that a coherent symbol detector must compensate for the channel phase shift, which means that the weight factor w_0 should be set to be proportional to $\text{sgn}\{\alpha_0\}$ before passing $y(n)$ through a thresholder. There are four pairs of possible values for $(s(n),s(n-1))$, resulting in

$$\begin{aligned}y_s(n)|(+1,+1)&=-y_s(n)|(-1,-1)\\ &=|\alpha_0|\sqrt{\mathcal{E}_s}R_p(\epsilon)\end{aligned} \tag{9}$$

$$\begin{aligned}y_s(n)|(+1,-1)&=-y_s(n)|(-1,+1)\\ &=|\alpha_0|\sqrt{\mathcal{E}_s}R_p(\epsilon)\left(1-\frac{2N_\epsilon}{N_f}\right).\end{aligned} \tag{10}$$

The conditional noisy output $y(n)$ is Gaussian with mean one of (9) and (10) and variance $\mathcal{N}_o/2$. Since $s(n)$ is i.i.d. with equal probabilities, the average BER is given by

$$\begin{aligned}P_e(N_\epsilon,\epsilon|\alpha_0)&=Pr\,(y(n)<0|s(n)=1)\\ &=\frac{1}{2}Pr(y(n)<0|(1,1))+\frac{1}{2}Pr(y(n)<0|(1,-1))\\ &=\frac{1}{2}Q\left(\sqrt{\frac{2\alpha_0^2\mathcal{E}_s}{\mathcal{N}_o}R_p^2(\epsilon)}\right)\\ &\quad+\frac{1}{2}Q\left(\sqrt{\frac{2\alpha_0^2\mathcal{E}_s}{\mathcal{N}_o}R_p^2(\epsilon)\left(1-\frac{2N_\epsilon}{N_f}\right)^2}\right)\end{aligned} \tag{11}$$

where $Q(x):=(1/\sqrt{2\pi})\int_{-\infty}^{x}e^{-u^2/2}du$ is the complementary error function. In a special case, the BER under perfect timing is given by $P_e(0,0|\alpha_0)=Q(\sqrt{2\alpha_0^2\mathcal{E}_s/\mathcal{N}_o})$, as expected.

The following can be deduced from (11).

- A mismatch in ϵ decides the portion of pulse energy collected by the correlator. When the tracking error $\epsilon\geq T_p$, it results in $R_p(\epsilon)=0$ and $P_e=1/2$. Hence, tracking is very critical in AWGN and flat fading channels. Sensitivity to the tracking error ϵ depends not only on the pulse duration T_p but also on the pulse shape via $R_p^2(\epsilon)$.
- A mismatch in N_ϵ introduces ISI and decides the portions of the received sample energy that are contributed from $s(n)$ and $s(n-1)$ via the ratio N_ϵ/N_f. The worst-case acquisition error occurs when $N_\epsilon=\lfloor N_f/2\rfloor$ ($\lfloor\cdot\rfloor$ denotes integer floor), which leads to

$$\begin{aligned}&P_e\left(\left\lfloor\frac{N_f}{2}\right\rfloor,\epsilon|\alpha_0\right)\\ &\quad=\begin{cases}\frac{1}{2}Q\left(\sqrt{\frac{2\alpha_0^2\mathcal{E}_s}{\mathcal{N}_o}R_p^2(\epsilon)}\right)+\frac{1}{4}, & N_f\text{ is even}\\ \frac{1}{2}Q\left(\sqrt{\frac{2\alpha_0^2\mathcal{E}_s}{\mathcal{N}_o}R_p^2(\epsilon)}\right)\\ \quad+\frac{1}{2}Q\left(\sqrt{\frac{2\alpha_0^2\mathcal{E}_s}{\mathcal{N}_o}\frac{R_p^2(\epsilon)}{N_f^2}}\right), & N_f\text{ is odd.}\end{cases}\end{aligned} \tag{12}$$

This can be understood by observing that when $N_\epsilon\leq N_f/2$, $s(n)$ is the primary contributor to $y_s(n)$, while $s(n-1)$ dominates when $N_\epsilon\geq N_f/2$. Since decisions are always made on the stronger symbol component, the BER sensitivity to N_ϵ is symmetric around $N_f/2$. With the signal energy reduction of $(1-2N_\epsilon/N_f)^2$ in (11), the sensitivity to acquisition

is reminiscent of the timing mismatch effect of a narrowband AWGN system with a rectangular pulse shaper of duration $N_f T_f$ [15].

These analytic expressions for UWB transmissions over AWGN channels are illustrated in Fig. 3. The following parameters are used: $\mathcal{E}_s/\mathcal{N}_o = 8$ dB, $N_f = 10$, $T_f = 10$ ns, and $T_p = 1$ ns. Note that the energy per pulse is constrained to be very low in UWB settings, but the effective SNR per symbol $\mathcal{E}_s/\mathcal{N}_o$ is typically set at a moderate level via choosing a large N_f in order to provide reliable symbol detection. The BER is plotted versus the normalized timing error T_f for the commonly used Gaussian monocycle[2] $p(t) = (1 - 4\pi t^2/\nu^2)\exp(-2\pi t^2/\nu^2)$ [2], where $\nu = 0.43$ ns, to yield $T_p = 1$ ns. The BER degradation features a gradual contour due to the frame-level acquisition error, whereas the actual performance exhibits sharp edges (one every T_f s) since the tracking error is strictly limited to the ultra-short pulse duration.

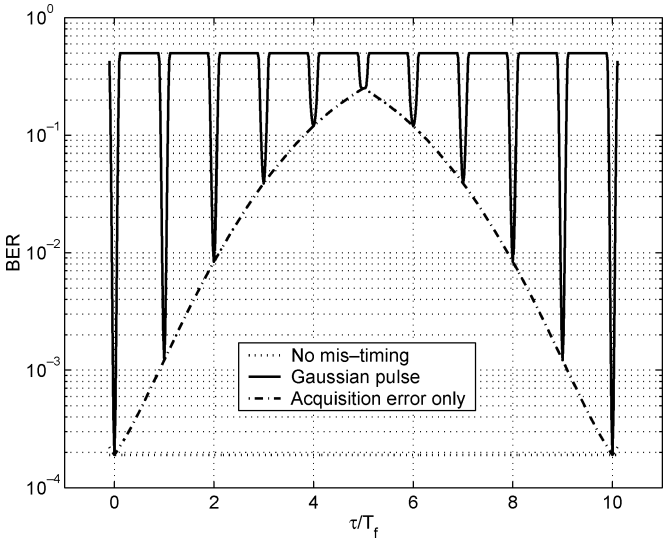

Fig. 3. BER performance for a direct-path AWGN channel. No TH.

B. TH PAM Transmissions Over AWGN Channels

In the presence of TH, $y_s(n)$ has the same form as in (6), but the argument Λ_p becomes $\Lambda_p = (k-n)N_f T_f + (i-j)T_f + (c(i) - c(j))T_c + N_\epsilon T_f + \epsilon$, where $c(i) \in [0, N_c - 1]$. As with (7) and (8), we analyze the constraints on the nontrivial triplets (k, i, j) and simplify $y_s(n)$ to (see Appendix I-A)

$$y_s(n) = w_0\alpha_0\sqrt{\mathcal{E}_s}s(n)\sum_{q=0}^{1}\sum_{j=N_\epsilon+q}^{N_f-1}\frac{R_p\left(\Lambda_p(j,q)\right)}{N_f} + w_0\alpha_0\sqrt{\mathcal{E}_s}s(n-1)\sum_{q=0}^{1}\sum_{j=0}^{N_\epsilon+q-1}\frac{R_p\left(\Lambda_p(j,q)\right)}{N_f} \quad (13)$$

where $\Lambda_p(j,q) := (c(j - N_\epsilon - q) - c(j))T_c + \epsilon - qT_f$. The decision statistic $y_s(n)$ depends on the TH code through Λ_p. Next, we will see that TH expands the allowable tracking mismatch ϵ and aggravates the BER degradation to acquisition mismatch.

TH sequences are pseudo-random (deterministic and periodic) or random. Since N_f is typically large (in the order of 100), the TH codes in both cases can be well modeled as being independent and uniformly distributed over $[0, N_c - 1]$. Correspondingly, the distribution of the code difference, which controls $\Lambda_p(j,q)$, is

$$P_r\left\{(c(j - N_\epsilon - q) - c(j))\,T_c = mT_c\right\} = \frac{1}{N_c}\left(1 - \frac{|m|}{N_c}\right) \quad N_\epsilon + q \neq 0 \quad (14)$$

where $m \in [-(N_c - 1), (N_c - 1)]$. Any of these $2N_c - 1$ values of m may appear in the summands of (13), resulting in $\Lambda_p = mT_c + \epsilon - qT_f$. If there exists a pair (m, q) such that $\Lambda_p \in (-T_p, T_p)$, some summands in (13) will be nonzero with certain probability, given that the tracking error is confined to $\epsilon = \Lambda_p - mT_c + qT_f \in (-T_p - mT_c + qT_f, T_p - mT_c + qT_f)$. To satisfy $\Lambda_p \in (-T_p, T_p)$, we observe that the nontrivial values for m differ, depending on q. When $q = 0$, $\Lambda_p = mT_c + \epsilon > mT_c - T_p$ is greater than $T_c - T_p > T_p$, for $m \geq 1$. Hence, the constraint $\Lambda_p < T_p$ implies that $m \leq 0$, which results in $(N_c + 1)$ nonoverlapping bins for the allowable values of $\epsilon : \mathcal{R}_0 := \cup\{(-mT_c - T_p, -mT_c + T_p)\}_{m=-(N_c-1)}^{0}$. Similarly, when $q = 1$, $\Lambda_p = mT_c + \epsilon - T_f < mT_c - T_p$, which implies $m \geq 1$, the allowable range for ϵ contains N_c nonoverlapping bins $\mathcal{R}_1 := \cup\{(T_f - mT_c - T_p, T_f - mT_c + T_p)\}_{m=1}^{N_c-1}$. With the use of TH, the allowable range for the tracking error ϵ to yield nonzero $R_p(\cdot)$ values in (13), and thus to ensure energy capture, is expanded to a total of $(2N_c - 1)$ bins, each of duration $2T_p$.

A special case arises when $N_\epsilon = 0$. Setting $N_\epsilon = 0$ in (13), the signal component $y_s(n)$ is reduced to

$$y_s(n) = w_0\alpha_0\sqrt{\mathcal{E}_s}\left(s(n)\frac{1}{N_f}\sum_{j=1}^{N_f-1}R_p\left(\Lambda_p(j,1)\right) + s(n)R_p(\epsilon) + s(n-1)\frac{1}{N_f}R_p\left(\Lambda_p(0,1)\right)\right). \quad (15)$$

When $\epsilon \in \mathcal{R}_1$, the last two terms survive, and ISI shows up. When $\epsilon \in (-T_p, T_p)$, only the first term remains, and no ISI emerges. This implies that, even with perfect acquisition, ambiguity on symbol transmission (or ISI) may be present due to TH because tracking errors beyond the interval $(-T_p, T_p)$ may result in nonzero $R_p(\Lambda_p)$.

Assume now that these $(2N_c - 1)$ bins are mutually exclusive.[3] The value of ϵ picks out a unique pair (m_o, q_o), if any, such that $\epsilon \in (-T_p - m_oT_c + q_oT_f, T_p - m_oT_c + q_oT_f)$. The decision statistic is then decided by how many out of the N_f code differences in (13) are equal to m_o. To answer this, let us introduce the notation $I_{j,q}(m) := \delta(m - (c(j - N_\epsilon - q) - c(j)))$, where

[2]Widely used in conventional impulse radios, the monocycle does not comply with the spectral mask recently released by the FCC. Nevertheless, we choose it in our numerical simulations for its wide recognition thus far. This choice does not compromise the usefulness of our simulations because the BER performance of a UWB radio is largely determined by the temporal properties of the pulse through the autocorrelation function $R_p(\cdot)$. At a very low duty cycle, the pulse bandwidth (and thus the pulse duration) affects the BER sensitivity to mistiming more than the actual spectral shape.

[3]The subregions in $\mathcal{R}_0$ and $\mathcal{R}_1$ are nonoverlapping when setting $T_c \geq 2T_p$. Deriving the BER is more complicated when $T_p < T_c \leq 2T_p$, but the same approach of analysis applies.

$\delta(\cdot)$ is Kronecker's Delta. Equation (13) can then be rewritten as

$$y_s(n) = w_0\alpha_0\sqrt{\mathcal{E}_s}s(n)\sum_{j=N_\epsilon+q_o}^{N_f-1} I_{j,q_o}(m_o) \times \frac{R_p(m_oT_c+\epsilon-q_oT_f)}{N_f} + w_0\alpha_0\sqrt{\mathcal{E}_s}s(n-1) \times \sum_{j=0}^{N_\epsilon+q_o-1} I_{j,q_o}(m_o)\frac{R_p(m_oT_c+\epsilon-q_oT_f)}{N_f}. \quad (16)$$

Let $\rho_0(k_0)$ denote the probability that the event $I_{j,q_o}(m_o)=1$ occurs k_0 times in the $N_f-N_\epsilon-q_o$ summands associated with $s(n)$ in (16). With $C_k^N := N!/k!(N-k)!$, it follows from (14) that for $k_0 \in [0, N_f-N_\epsilon-q_o]$

$$\rho_0(k_0)=\begin{cases} C_{k_0}^{N_f-N_\epsilon-q_o}\left(\frac{N_c-|m_o|}{N_c^2}\right)^{k_0} \times\left(1-\frac{N_c-|m_o|}{N_c^2}\right)^{N_f-N_\epsilon-q_o-k_0}, & N_\epsilon+q_o\neq 0 \\ \delta\left(k_0-(N_f-N_\epsilon-q_o)\right)\delta(m_o), & N_\epsilon+q_o=0. \end{cases} \quad (17)$$

Similarly, let $\rho_1(k_1)$ denote the probability that the event $I_{j,q_o}(m_o)=1$ occurs k_1 times in the $N_\epsilon+q_o$ summands associated with $s(n-1)$ in (16). We have $\rho_1(k_1) = C_{k_1}^{N_\epsilon+q_o}(N_c-|m_o|/N_c^2)^{k_1}(1-(N_c-|m_o|/N_c^2))^{N_\epsilon+q_o-k_1}$ for $k_1\in[0,N_\epsilon+q_o]$ when $N_\epsilon+q_o\neq 0$, and $\rho_1(k_1)=\delta(k_1)\delta(m_o)$ for $N_\epsilon+q_o=0$. In all, $y_s(n)$ takes on the following value with probability $\rho_0(k_0)\cdot\rho_1(k_1)$:

$$y_s(n) = w_0\alpha_0\sqrt{\mathcal{E}_s}R_p(m_oT_c+\epsilon-q_oT_f) \times\left(s(n)\frac{k_0}{N_f}+s(n-1)\frac{k_1}{N_f}\right) \text{ for } k_0\in[0,N_f-N_\epsilon-q_o], k_1\in[0,N_\epsilon+q_o]. \quad (18)$$

The procedure for analyzing the BER is as follows: If $\epsilon\notin(\mathcal{R}_0\cup\mathcal{R}_1)$, it falls outside these $(2N_c-1)$ bins, which results in $y(n)=v(n)$ and $P_e=0.5$. When $\epsilon\in(\mathcal{R}_0\cup\mathcal{R}_1)$, a unique pair (m_o,q_o) can be identified, and (18) applies. To evaluate $Pr(y(n)<0|s(n)=1)$ in a coherent detector (i.e., $w_0=\text{sgn}\{\alpha_0\}$), we note that $y_s(n)$ conditioned on $(s(n),s(n-1))$ is given by

$$y_s(n)|(1,\pm1) = |\alpha_0|\sqrt{\mathcal{E}_s}R_p(m_oT_c+\epsilon-q_oT_f)\frac{k_0\pm k_1}{N_f}. \quad (19)$$

Depending on $s(n-1)$, k_0, and k_1, $y_s(n)$ conditioned on $s(n)=1$ may take $(N_f+N_\epsilon+q_o)$ possible values. Conditioned on (k_0,k_1), the BER is given by

$$P_e(k_0,k_1|\alpha_0) = \frac{1}{2}Q\left(\sqrt{\frac{2\alpha_0^2\mathcal{E}_s}{\mathcal{N}_o}R_p^2(m_oT_c+\epsilon-q_oT_f)\left(\frac{k_0+k_1}{N_f}\right)^2}\right) + \frac{1}{2}Q\left(\sqrt{\frac{2\alpha_0^2\mathcal{E}_s}{\mathcal{N}_o}R_p^2(m_oT_c+\epsilon-q_oT_f)}\left(\frac{k_0-k_1}{N_f}\right)\right). \quad (20)$$

Hence, the BER averaged over all possible (k_0,k_1) pairs is given by

$$P_e(N_\epsilon,\epsilon|\alpha_0) = \sum_{k_0=0}^{N_f-N_\epsilon-q_o}\sum_{k_1=0}^{N_\epsilon+q_o}\rho_0(k_0)\rho_1(k_1)P_e(k_0,k_1|\alpha_0). \quad (21)$$

Again, the result applies to $N_\epsilon\le\lfloor N_f/2\rfloor$, and the BER is symmetric in N_ϵ around $N_f/2$. The BER performance without timing mismatch remains unchanged in the TH case: $P_e(0,0|\alpha_0)=Q(\sqrt{2\alpha_0^2\mathcal{E}_s/\mathcal{N}_o})$.

The following observations are made on the TH case with a sliding correlator.

- Acquisition becomes very critical. When $N_\epsilon\neq 0$, the reduction in receive signal energy is decided by $(1/N_f)\sum_{j=N_\epsilon+q_o}^{N_f-1}I_{j,q_o}(m_o)$, which indicates the chance that the pulses in misaligned frames happen to be picked out by hopping codes of different frames. The large error terms in (21) correspond to small values for k_0 and k_1, which unfortunately force large probabilities $\rho_0(k_0)\rho_1(k_1)$, thus dominating the average BER.
- Mistracking tolerance is seemingly enhanced by TH. The allowable range for ϵ is now increased from $(-T_p,T_p)$ to $(2N_c-1)$ bins of $2T_p$ seconds each. On the other hand, due to the more stringent requirement on acquisition, the enhanced tracking range does not bring real improvement in BER robustness. When $N_\epsilon=0$, the tracking error is still limited to $(-T_p,T_p)$ to avoid ISI [c.f. (15)]. When $N_\epsilon\neq 0$, there is only a small chance of energy capture when the correlator coincides with the transmitted pulses after random hopping.

Overall, although TH alleviates the need for tracking, the BER performance is considerably compromised in the presence of acquisition errors. The effect of TH on a direct-path channel is confirmed in Fig. 4, which adopts the same system parameters as in the absence of TH. TH codes of different lengths ($N_c=2,5$) are evaluated, where a larger N_c may accommodate more users. With an increase in N_c, there is a larger number of weaker spikes in the BER curves, which illustrates that the BER degradation due to acquisition errors is aggravated.

C. PAM Transmissions Over Dense Multipath Channels

In a dense-multipath channel, we have $L\gg 1$. We start with a symbol-rate sliding correlator by taking $L'=0$ in (5). The resulting $y_s(n)$ becomes

$$y_s(n) = \sqrt{\mathcal{E}_s}\sum_{k=0}^{\infty}s(k)\sum_{i=0}^{N_f-1}\sum_{j=0}^{N_f-1}w_0 \times\sum_{l=0}^{L}\frac{\alpha_l R_p((k-n)N_fT_f+(i-j)T_f+N_\epsilon T_f+\epsilon+\tau_{l,0})}{N_f}. \quad (22)$$

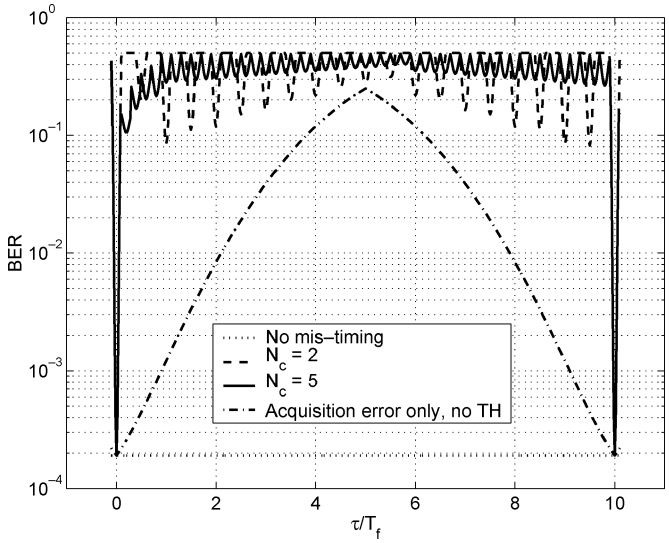

Fig. 4. BER for a direct-path AWGN channel. With TH.

Carrying over the analysis on the constraints of nontrivial triplets (k,i,j), (22) can be simplified to (see Appendix I-B)

$$y_s(n)=\sqrt{\mathcal{E}_s}w_0\sum_{l=0}^{L}\sum_{q=0}^{1}\alpha_l R_p(\epsilon+\tau_{l,0}-qT_f)\cdot\left(s(n)\left(1-\frac{N_\epsilon+q}{N_f}\right)+s(n-1)\frac{N_\epsilon+q}{N_f}\right). \quad (23)$$

To yield nonzero R_p in (23), we observe that $q=0$ when $\epsilon\in[-T_p,T_p)$ and $q=1$ otherwise, regardless of N_ϵ. This implies that, even with perfect acquisition, ISI may be present due to multipath when tracking errors are beyond the interval $[-T_p,T_p)$. Similar symbol ambiguity (that is, unexpected ISI) induced by signal spreading has been observed due to TH.

Conditioned on $(s(n)=1,s(n-1)=\pm1)$, $y(n)$ is given by

$$y(n)|(1,1)=\sqrt{\mathcal{E}_s}w_0\sum_{l=0}^{L}\sum_{q=0}^{1}\alpha_l R_p(\epsilon+\tau_{l,0}-qT_f)+v(n) \quad (24)$$

$$y(n)|(1,-1)=\sqrt{\mathcal{E}_s}w_0\sum_{l=0}^{L}\sum_{q=0}^{1}\alpha_l R_p(\epsilon+\tau_{l,0}-qT_f)\times\left(1-\frac{2N_\epsilon+2q}{N_f}\right)+v(n). \quad (25)$$

Sufficient energy capture is critical to detecting signals scattered by dense multipath channels. Let $\mathcal{E}_\alpha(N_\epsilon,\epsilon|\{\alpha_l\}_{l=0}^L)$ denote the portion of path energy that is collected by a receiver under both acquisition and tracking errors, and $\mathcal{E}_\alpha(\epsilon|\{\alpha_l\}_{l=0}^L)$ as the received path energy subject to tracking error only. For a coherent correlator, $\mathcal{E}_\alpha(\epsilon|\{\alpha_l\}_{l=0}^L)$ and $\mathcal{E}_\alpha(N_\epsilon,\epsilon|\{\alpha_l\}_{l=0}^L)$ can be deduced from (24) and (25), respectively, noting that transmission of identical consecutive symbols in (24) reduces the impact of acquisition errors. Setting w_0 to compensate for the phase shift of the aggregate channel described in the summation over l, we have $\mathcal{E}_\alpha(\epsilon|\{\alpha_l\}_{l=0}^L)=\left(\sum_{l=0}^{L}\sum_{q=0}^{1}\alpha_l R_p(\epsilon+\tau_{l,0}-qT_f)\right)^2$ and $\mathcal{E}_\alpha(N_\epsilon,\epsilon|\{\alpha_l\}_{l=0}^L)=\left(\sum_{l=0}^{L}\sum_{q=0}^{1}\alpha_l R_p(\epsilon+\tau_{l,0}-qT_f)(1-2(N_\epsilon+q/N_f))\right)^2$. Accordingly, the BER is given by

$$\begin{aligned}P_e&\left(N_\epsilon,\epsilon|\{\alpha_l\}_{l=0}^L\right)\\&=Pr\left(y(n)<0|s(n)=1\right)\\&=\frac{1}{2}Pr\left(y(n)<0|(1,1)\right)+\frac{1}{2}Pr\left(y(n)<0|(1,-1)\right)\\&=\frac{1}{2}Q\left(\sqrt{\frac{2\mathcal{E}_s\mathcal{E}_\alpha\left(\epsilon|\{\alpha_l\}_{l=0}^L\right)}{\mathcal{N}_o}}\right)\\&\quad+\frac{1}{2}Q\left(\sqrt{\frac{2\mathcal{E}_s\mathcal{E}_\alpha\left(N_\epsilon,\epsilon|\{\alpha_l\}_{l=0}^L\right)}{\mathcal{N}_o}}\right).\end{aligned} \quad (26)$$

Note that the channel taps picked by the summations in $\mathcal{E}_\alpha(\epsilon|\{\alpha_l\}_{l=0}^L)$ and $\mathcal{E}_\alpha(N_\epsilon,\epsilon|\{\alpha_l\}_{l=0}^L)$ are determined by ϵ. In a dense-multipath environment where the tap delay spacing is small, i.e., $\tau_{l+1}-\tau_l\le 2T_p$ for any l, at least one of the l's will result in $\epsilon+\tau_{l,0}-qT_f\in(-T_p,T_p)$ for some $q\in[0,1]$. Therefore, the correlator always collects signal energy for any $\epsilon\in[-T_p,T_f-T_p)$. On the other hand, when $\tau_{l+1}-\tau_l\ge T_p$, which is a reasonable constraint since T_p is the minimum path resolution time, there are only up to two possible values of l that will contribute nonzero summands for any ϵ. Compared with the total path energy $\sum_{l=0}^{L}\alpha_l^2$, the energy collected by a sliding correlator is substantially reduced, which necessitates exploitation of diversity using RAKE combiners.

Let us consider a RAKE receiver constructed with perfect channel knowledge. When TH is not employed, the output of a RAKE can be obtained from (5) by taking out the TH terms

$$y_s(n)=\sqrt{\mathcal{E}_s}\sum_{k=0}^{\infty}s(k)\sum_{i=0}^{N_f-1}\sum_{j=0}^{N_f-1}\sum_{l=0}^{L}\sum_{l'=0}^{L'}\frac{w_{l'}\alpha_l}{N_f}\cdot R_p\left((k-n)\times N_fT_f+(i-j)T_f+N_\epsilon T_f+\epsilon+\tau_{l,0}-\tilde{\tau}_{l',0}\right). \quad (27)$$

Similar to (23), $y_s(n)$ can be simplified to (see Appendix I-B)

$$y_s(n)=\sqrt{\mathcal{E}_s}\sum_{l=0}^{L}\sum_{l'=0}^{L'}\sum_{q=0}^{1}w_{l'}\alpha_l R_p(\epsilon+\tau_{l,0}-\tilde{\tau}_{l',0}-qT_f)\cdot\left(s(n)\left(1-\frac{N_\epsilon+q}{N_f}\right)+s(n-1)\frac{N_\epsilon+q}{N_f}\right). \quad (28)$$

By inspecting $y_s(n)$ conditioned on $(s(n),s(n-1))$, we obtain the energy capture indices for a RAKE receiver:

$$\mathcal{E}_\alpha\left(\epsilon|\{\alpha_l\}_{l=0}^L\right)=\left(\sum_{l'=0}^{L'}w_{l'}\sum_{l=0}^{L}\alpha_l\sum_{q=0}^{1}R_p(\epsilon+\tau_{l,0}-\tilde{\tau}_{l',0}-qT_f)\right)^2 \quad (29)$$

$$\mathcal{E}_\alpha\left(N_\epsilon,\epsilon|\{\alpha_l\}_{l=0}^L\right)=\left(\sum_{l'=0}^{L'}w_{l'}\sum_{l=0}^{L}\alpha_l\sum_{q=0}^{1}R_p(\epsilon+\tau_{l,0}-\tilde{\tau}_{l',0}-qT_f)\cdot\left(1-\frac{2(N_\epsilon+q)}{N_f}\right)\right)^2. \quad (30)$$

Substituting (29) and (30) into (26), we can readily obtain the BER for the RAKE receiver.

Time hopping affects the robustness of RAKE reception to mistiming. Different from the AWGN case, we do not assume any probabilistic model for the TH codes here but carry out our analysis conditioned on the TH codes. In the AWGN case, it is imperative to study the allowable range of the tracking error; therefore, a statistical viewpoint is instrumental. In the dense multipath case, on the other hand, a receiver will always match to some signal paths of the signal component, regardless of any tracking error, but the energy capture may not be sufficient under mistiming. TH codes merely change the path positions and the associated RAKE weights but not the number of paths collected by the receiver. Hence, a statistical model for the TH codes is not well motivated. With this in mind, we carry over the analysis on nontrivial triplets in (5) for the TH case and reach a simplified version of the decision statistic as follows (see Appendix I-C):

$$\begin{aligned} y_s(n) &= \sqrt{\mathcal{E}_s}s(n) \\ &\quad \times \sum_{l=0}^{L}\sum_{l'=0}^{L'}\sum_{q=-1}^{2}\left(\frac{1}{N_f}\sum_{j=N_\epsilon+q}^{N_f-1} w_{l'}\alpha_l R_p(\Lambda_p(j,l,l',q))\right) \\ &\quad + \sqrt{\mathcal{E}_s}s(n-1) \\ &\quad \times \sum_{l=0}^{L}\sum_{l'=0}^{L'}\sum_{q=-1}^{2}\left(\frac{1}{N_f}\sum_{j=0}^{N_\epsilon+q-1} w_{l'}\alpha_l R_p(\Lambda_p(j,l,l',q))\right) \end{aligned} \tag{31}$$

where $\Lambda_p(j,l,l',q) := (c(j-N_\epsilon-q)-c(j))T_c+\epsilon+\tau_{l,0}-\tilde{\tau}_{l',0}-qT_f$. For given j and q, there is only one code difference m out of $(2N_c-1)$ possible values per realization. Compared with the no-TH case in (28), it is now the tracking error $mT_c+\epsilon$ that determines the RAKE fingers l' to be matched to each path l. The BER can be derived as (32), shown at the bottom of the page.

In contrast to a direct-path channel, dense multipath propagation implies different timing tolerances.

- For a sliding correlator, a dense-multipath channel imposes less stringent requirements on tracking, allowing $\epsilon \in [-T_p, T_f - T_p)$. On the other hand, due to the energy spreading over multiple paths, the weak energy-capture capability discourages its use in power-limited UWB transmissions.
- For RAKE reception under fixed channel realizations, signal detection is robust to tracking errors. When $\tilde{\tau}_{l',0} = \tau_{l',0}$, $\forall l'$, it follows from (28) that for any $\epsilon \in [-T_p, T_f - T_p)$, every path $l \in [0, L]$ will be picked at most by two RAKE fingers l', such that $\epsilon + \tau_{l,0} - \tilde{\tau}_{l',0} - qT_f \in (-T_p, T_p)$.
- When TH is employed, the energy capture is similar to the no-TH case, except that the TH codes alter the taps picked out. Such a shuffling of taps is equivalent to noise averaging and, thus, induces diversity even when only a simple correlator is used.

This assessment is verified via analytical evaluation depicted in Fig. 5. In the dense-multipath channel used, the path delays are taken to be $\tau_l = \tau_0 + lT_p$, $0 \le l \le \lfloor (T_f - 2T_p)/T_p \rfloor$, and the path gains are assumed to fall off exponentially according to the profile $E\{\alpha_l^2\} = \mathcal{E}_0 e^{-\lambda l}$, where $\mathcal{E}_0$ is a scaling factor to normalize the total multipath power spread to unity (i.e., $\sum_{l=0}^{L} E\{\alpha_l^2\} = 1$), and $\lambda = 2/3$ is the decay factor [5]. For the time being, we assume no fading, i.e., $|\alpha_l| = \sqrt{E\{\alpha_l^2\}}$ with its sign randomly chosen between ± 1 with equal probabilities. We depict the BER performance of a sliding correlator (RAKE-1: $L' = 0$) and an equal gain combiner (RAKE-EGC: $\tilde{\tau}_l = \tau_l$, $L' = L$) to illustrate the drastically different sensitivity in dense multipath compared with a direct path. In the absence of TH, the RAKE-1 receiver only picks out a very small number of paths, where the time locations of the contributing paths are determined by ϵ. As a result, the BER performance of RAKE-1 exhibits a similar pattern as the channel power delay profile. It may perform well when it happens to catch strong paths at certain ϵ but generally is ineffective in energy capture. The RAKE-EGC receiver, on the other hand, averages out the received energy from all paths within a frame using equal weights; thus, the BER performance is relatively insensitive to the tracking error. When TH is present, RAKE-1 does not work well because it can no longer catch strong paths in all frames, regardless of ϵ. Meanwhile, the performance advantage of RAKE-EGC over RAKE-1 is more pronounced only when $N_\epsilon = 0$ but less obvious when there exists any acquisition error. The more interesting maximum ratio combining (MRC) receiver will be discussed for fading channels in Part II of this paper [6].

Thus far, we have established a unifying signal model for analyzing the detection performance of a correlation-based receiver under mistiming. Timing tolerances in different propagating environments have been discussed based on fixed channel realizations. In Part II of this paper [6], we will present a unifying approach for BER performance analysis under mistiming for random fading channels, along with corroborating simulations and summarizing remarks.

$$\begin{aligned} &P_e\left(N_\epsilon,\epsilon|\{\alpha_l\}_{l=0}^{L},\{c(j)\}_{j=0}^{N_f-1}\right) \\ &\quad = \frac{1}{2}Q\left(\sqrt{\frac{2\mathcal{E}_s}{\mathcal{N}_o}\left(\sum_{l=0}^{L}\sum_{l'=0}^{L'}\sum_{q=-1}^{2}\frac{1}{N_f}\sum_{j=0}^{N_f-1} w_{l'}\alpha_l R_p\left(\Lambda_p(j,l,l',q)\right)\right)^2}\right) \\ &\qquad + \frac{1}{2}Q\left(\sqrt{\frac{2\mathcal{E}_s}{\mathcal{N}_o}}\left(\sum_{l=0}^{L}\sum_{l'=0}^{L'} w_{l'}\alpha_l \sum_{q=-1}^{2}\frac{1}{N_f}\left(\sum_{j=N_\epsilon+q}^{N_f-1} R_p\left(\Lambda_p(j,l,l',q)\right) - \sum_{j=0}^{N_\epsilon+q-1} R_p\left(\Lambda_p(j,l,l',q)\right)\right)\right)\right). \end{aligned} \tag{32}$$

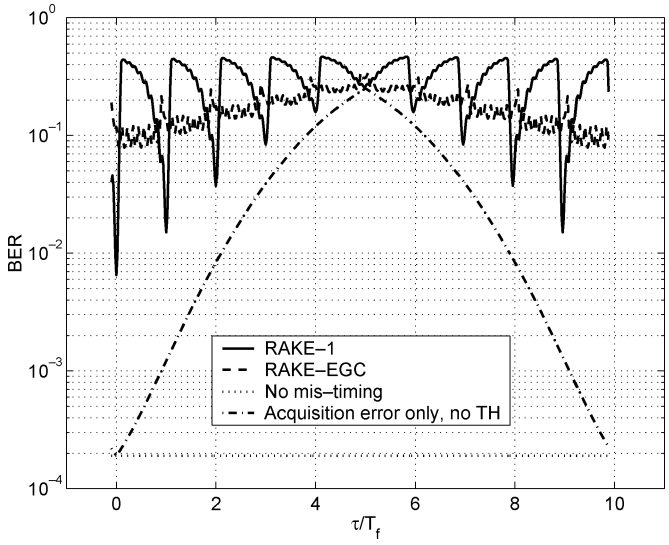

(a)

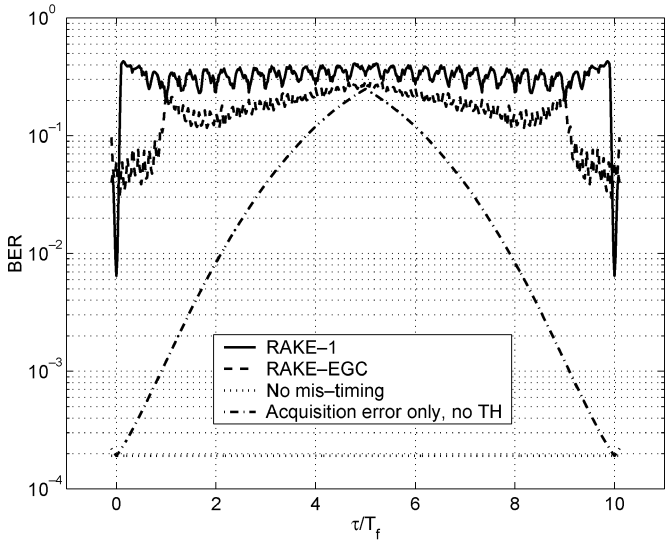

(b)

Fig. 5. BER performance for a multipath AWGN channel. (a) No TH. (b) With TH ($N_c = 3$).

APPENDIX I
SIMPLIFIED DETECTION STATISTICS

In this Appendix, we detail the steps used to simplify the decision statistic $y_s(n)$ for various operating conditions under the constraints on nontrivial triplets (k, i, j).

A. TH PAM Transmissions Over AWGN Channels

For TH PAM transmissions over AWGN channels, $y_s(n)$ is given by (33), shown at the bottom of the page. Similar to (7), the triplet (k, i, j) contributes a nonzero $R_p(\cdot)$ in (33) only when there exists an integer q such that

$$(k-n)N_f + N_\epsilon + (i-j) + q = 0; \tag{34}$$

$$(c(i) - c(j))\,T_c + \epsilon - qT_f \in (-T_p, T_p). \tag{35}$$

Note that $(c(i) - c(j))T_c \in [-T_f + T_c, T_f - T_c)$, and $\epsilon \in [-T_p, T_f - T_p)$, which dictates $(c(i) - c(j))T_c + \epsilon \in [-T_f + T_c - T_p, 2T_f - T_c - T_p)$. Hence, it can be seen from (35) that the allowable values for q are 0, 1. Meanwhile, since $N_\epsilon + (i-j) + q \in [-(N_f - 1), 2N_f - 1)]$, the allowable values for $k - n$ in (34) are confined to $(k-n)N_f \in [-(2N_f - 1), (N_f - 1)]$, which leads to $k - n \in \{0, -1\}$. Moreover, $i = j - N_\epsilon - q - (k-n)N_f$ is confined to $[0, N_f - 1]$. Therefore, if $j \in [0, N_\epsilon] + q - 1]$, then $i = j - N_\epsilon - q$ and $k = n$. Furthermore, when $j \in [N_\epsilon + q, N_f - 1]$, we have that $i = j - N_\epsilon - q - N_f$, and $k = n - 1$. In summary

$$\begin{aligned} y_s(n) &= \alpha_0\sqrt{\mathcal{E}_s}s(n-1) \\ &\quad\times\sum_{q=0}^{1}\sum_{j=0}^{N_\epsilon+q-1}\frac{R_p(\left(c(j-N_\epsilon-q+N_f)-c(j)\right)T_c+\epsilon-qT_f)}{N_f} \\ &\quad+\alpha_0\sqrt{\mathcal{E}_s}s(n) \\ &\quad\times\sum_{q=0}^{1}\sum_{j=N_\epsilon+q}^{N_f-1}\frac{R_p(\left(c(j-q-N_\epsilon)-c(j)\right)T_c+\epsilon-qT_f)}{N_f}. \end{aligned} \tag{36}$$

Because the TH code is symbol periodic, we have $c(j - N_\epsilon - q + N_f) = c(j - N_\epsilon - q)$.

B. TH-Free PAM Over Dense Multipath Channels

For dense multipath without the use of TH, the decision statistic is

$$\begin{aligned} y_s(n) &= \sqrt{\mathcal{E}_s}\sum_{k=0}^{\infty}s(k)\sum_{i=0}^{N_f-1}\sum_{j=0}^{N_f-1}\sum_{l=0}^{L}\alpha_l \\ &\quad\cdot\frac{R_p\left((k-n)N_fT_f + (i-j)T_f + N_\epsilon T_f + \epsilon + \tau_{l,0}\right)}{N_f}. \end{aligned} \tag{37}$$

Due to the narrow nonzero support of $R_p(\tau)$, we have

$$(k-n)N_fT_f + (i-j)T_f + N_\epsilon T_f + qT_f = 0; \tag{38}$$

$$\epsilon + \tau_{l,0} - qT_f \in (-T_p, T_p). \tag{39}$$

Since $\tau_{l,0} \in [0, T_f - 2T_p]$, we have

$$\epsilon + \tau_{l,0} - qT_f \in [-qT_f, (2-q)T_f - T_p) \quad \Rightarrow q = 0, 1 \tag{40}$$

$$\begin{aligned} (k-n)N_f = -(i-j) - N_\epsilon - q \in [-(2N_f-1), N_f-1] \\ \Rightarrow (k-n) \in \{0, -1\}; \end{aligned} \tag{41}$$

$$y_s(n) = \alpha_0\sqrt{E_s}\sum_{k=0}^{\infty}s(k)\sum_{i=0}^{N_f-1}\sum_{j=0}^{N_f-1}\frac{R_p\left((k-n)N_fT_f + (i-j)T_f + N_\epsilon T_f + (c(i)-c(j))\,T_c + \epsilon\right)}{N_f}. \tag{33}$$

$$i = j - N_\epsilon - q - (k-n)N_f \in [0, N_f - 1] \Rightarrow \begin{cases} \text{when } j \in [0, N_\epsilon + q - 1], & k = n - 1 \\ & i = j - N_\epsilon - q + N_f \\ \text{when } j \in [N_\epsilon + q, N_f - 1], & k = n, i = j - N_\epsilon - q. \end{cases} \tag{42}$$

Dissection on (40) reveals that $q = 0$ when $\epsilon \in [-T_p, T_p)$, and $q = 1$ otherwise. For a given ϵ, at most one q value contributes to nonzero correlation $R_p(\epsilon + \tau_l - qT_f)$ for any $\tau_{l,0} \in [0, T_f - 2T_p)$.

Using (40) and (41), (37) is simplified to

$$y_s(n) = \sqrt{\mathcal{E}_s} \sum_{q=0}^{1} (s(n)(N_f - N_\epsilon - q) + s(n-1)(N_\epsilon + q)) \cdot \sum_{l=0}^{L} \frac{\alpha_l R_p(\epsilon + \tau_{l,0} - qT_f)}{N_f}. \tag{43}$$

When RAKE reception is involved, the output of a RAKE combiner is given by (5) after taking out the TH terms

$$y_s(n) = \sqrt{\mathcal{E}_s} \sum_{k=0}^{\infty} s(k) \sum_{i=0}^{N_f-1} \sum_{j=0}^{N_f-1} \sum_{l=0}^{L} \sum_{l'=0}^{L'} \frac{w_{l'} \alpha_l}{N_f} \cdot R_p\left((k-n)N_f T_f + (i-j)T_f + N_\epsilon T_f + \epsilon + \tau_{l,0} - \tilde{\tau}_{l',0}\right). \tag{44}$$

Following the previous analysis, (38) still holds, whereas (39) is changed to $\epsilon + \tau_{l,0} - \tilde{\tau}_{l',0} - qT_f \in (-T_p, T_p)$. Taking into account that $\tau_{l,0} - \tilde{\tau}_{l',0} \in [-T_f + 2T_p, T_f - 2T_p]$, we have the following conditions for reaching nonzero summands in (44):

$$\epsilon + \tau_{l,0} - \tilde{\tau}_{l',0} - qT_f \in [-(1+q)T_f + T_p, (2-q)T_f - T_p) \Rightarrow q = 0, 1. \tag{45}$$

Since the possible values for q are the same as in (40), and (38) remains the same, the conditions on (k, i, j) are still described by (41) and (42).

C. TH PAM Over Dense Multipath Channels

In a dense multipath channel with TH, the output of a RAKE receiver is given by (5)

$$y_s(n) = \sqrt{\mathcal{E}_s} \sum_{k=0}^{\infty} s(k) \sum_{i=0}^{N_f-1} \sum_{j=0}^{N_f-1} \sum_{l=0}^{L} \sum_{l'=0}^{L'} \frac{w_{l'} \alpha_l}{N_f} \cdot R_p\left((k-n)N_f T_f + (i-j)T_f + (c(i) - c(j))T_c + N_\epsilon T_f + \epsilon + \tau_{l,0} - \tilde{\tau}_{l',0}\right). \tag{46}$$

Following the previous analysis, (38) still holds, whereas (39) is changed to $(c(i) - c(j))T_c + \epsilon + \tau_{l,0} - \tilde{\tau}_{l',0} - qT_f \in (-T_p, T_p)$.

Since $(c(i) - c(j))T_c \in [-T_f + T_c, T_f - T_c]$, and $\tau_{l,0} - \tilde{\tau}_{l',0} \in [-T_f + 2T_p, T_f - 2T_p]$, we have the following conditions for the summands in (46) to be nonzero:

$$\epsilon + (c(i) - c(j))T_c + \tau_{l,0} - \tilde{\tau}_{l',0} - qT_f \in [-(2+q)T_f + T_c + T_p, (3-q)T_f - T_c - 3T_p) \Rightarrow q \in [-1, 2] \tag{47}$$

$$(k-n)N_f = -(i-j) - N_\epsilon - q \in [-2N_f, N_f] \Rightarrow k - n \in [-2, 1] \tag{48}$$

$$i = j - N_\epsilon - q - (k-n)N_f \in [0, N_f - 1] \Rightarrow \begin{cases} \text{when } j \in [N_\epsilon + q, N_f - 1], & k = n, i = j - N_\epsilon - q; \\ \text{when } j \in [0, N_\epsilon + q - 1], & k = n - 1 \\ & i = j - N_\epsilon - q + N_f. \end{cases} \tag{49}$$

It is seen from (49) that when $k - n = 1, -2$, the constraints $i, j \in [0, N_f - 1]$ are violated. Therefore, the allowable range of $k - n$ is still confined to be $k - n = 0, -1$. In summary, we have

$$\begin{aligned} y_s(n) = \sqrt{\mathcal{E}_s} s(n) & \sum_{q=-1}^{2} \sum_{j=N_\epsilon+q}^{N_f-1} \sum_{l=0}^{L} \sum_{l'=0}^{L'} \frac{w_{l'} \alpha_l}{N_f} \\ & \cdot R_p\left((c(j - N_\epsilon - q) - c(j))T_c + \epsilon + \tau_{l,0} - \tilde{\tau}_{l',0} - qT_f\right) \\ & + \sqrt{\mathcal{E}_s} s(n-1) \sum_{q=-1}^{2} \sum_{j=0}^{N_\epsilon+q-1} \sum_{l=0}^{L} \sum_{l'=0}^{L'} \frac{w_{l'} \alpha_l}{N_f} \\ & \cdot R_p\left((c(j - N_\epsilon - q) - c(j))T_c + \epsilon + \tau_{l,0} - \tilde{\tau}_{l',0} - qT_f\right). \end{aligned} \tag{50}$$

It can be observed from (47) that when $(c(i) - c(j))T_c \geq 0$, $q = -1$ does not contribute to $y(n)$. Conversely, when $(c(i) - c(j))T_c \leq 0$, $q = 2$ does not contribute to $y(n)$.

REFERENCES

[1] F. Ramirez-Mireles, "On the performance of ultra-wide-band signals in Gaussian noise and dense multipath," *IEEE Trans. on Veh. Technol.*, vol. 50, no. 1, pp. 244–249, Jan. 2001.

[2] M. Z. Win and R. A. Scholtz, "Ultra wide bandwidth time-hopping spread-spectrum impulse radio for wireless multiple access communications," *IEEE Trans. Commun.*, vol. 48, no. 4, pp. 679–689, Apr. 2000.

[3] J. Foerster, E. Green, S. Somayazulu, and J. Leeper, "Ultra-wideband technology for short or medium range wireless communications," *Intel Corp. Tech. J.*, vol. Q2, 2001, [Online] Available: http://developer.intel.com/technology/itj.

[4] W. M. Lovelace and J. K. Townsend, "The effects of timing jitter and tracking on the performance of impulse radio," *IEEE J. Sel. Areas Commun.*, vol. 20, no. 12, pp. 1646–1651, Dec. 2002.

[5] J. Foerster, "The effects of multipath interference on the performance of UWB systems in an indoor wireless channel," in *Proc. Veh. Tech. Conf.*, 2001, pp. 1176–1180.

[6] Z. Tian and G. B. Giannakis, "BER sensitivity to mistiming in ultra-wideband impulse radios—Part II: Performance in fading channels," *IEEE Trans. Signal Process.*, vol. 53, no. 5, May 2005, to be published.

[7] IEEE 802.15 WPAN High Rate Alternative PHY Task Group 3a (TG3a)*http://www.ieee802.org/15/pub/TG3a.html* [Online]

[8] C. J. Le Martret and G. B. Giannakis, "All-digital impulse radio for wireless cellular systems," *IEEE Trans. Commun.*, vol. 50, no. 9, pp. 1440–1450, Sep. 2002.

[9] A. R. Forouzan, M. Nasiri-Kenari, and J. A. Salehi, "Performance analysis of ultra-wideband time-hopping spread spectrum multiple-access systems: Uncoded and coded schemes," *IEEE Trans. Wireless Commun.*, vol. 1, no. 4, pp. 671–681, Oct. 2002.

[10] R. Fleming, C. Kushner, G. Roberts, and U. Nandiwada, "Rapid acquisition for ultra-wideband localizers," in *Proc. IEEE Conf. UWB Syst. Technol.*, Baltimore, MD, May 2002, pp. 245–250.

[11] H. Lee, B. Han, Y. Shin, and S. Im, "Multipath characteristics of impulse radio channels," in *Proc. IEEE Veh. Technol. Conf.*, Tokyo, Japan, Spring 2000, pp. 2487–2491.

[12] A. A. M. Saleh and R. A. Valenzuela, "A statistical model for indoor multipath propagation," *IEEE J. Sel. Areas Commun.*, vol. JSAC-5, no. 2, pp. 128–137, Feb. 1987.
[13] D. Cassioli, M. Z. Win, and A. F. Molisch, "The UWB indoor channel: from statistical model to simulations," *IEEE J. Sel. Areas Commun.*, vol. 20, no. 8, pp. 1247–1257, Aug. 2002.
[14] M. Z. Win and R. A. Scholtz, "Characterization of UWB wireless indoor channels: a communication-theoretic view," *IEEE J. Sel. Areas Commun.*, vol. 20, no. 12, pp. 1613–1627, Dec. 2002.
[15] J. G. Proakis and M. Salehi, *Communication Systems Engineering*, Second ed. Englewood Cliffs, NJ: Prentice-Hall, 2002, Sect. 7.8: Symbol Synchronization.

Zhi Tian (M'98) received the B.E. degree in electrical engineering (automation) from the University of Science and Technology of China, Hefei, China, in 1994 and the M. S. and Ph.D. degrees from George Mason University, Fairfax, VA, in 1998 and 2000.

From 1995 to 2000, she was a graduate research assistant with the Center of Excellence in Command, Control, Communications, and Intelligence (C^3I) of George Mason University. Since August 2000, she has been an Assistant Professor with the Department of Electrical and Computer Engineering, Michigan Technological University, Houghton. Her current research focuses on signal processing for wireless communications, particularly on ultrawideband systems.

Dr. Tian serves as an Associate Editor for IEEE TRANSACTIONS ON WIRELESS COMMUNICATIONS. She received a 2003 NSF CAREER award.

Georgios B. Giannakis (F'97) received the Diploma in electrical engineering from the National Technical University of Athens, Athens, Greece, in 1981 and the M.Sc. degree in electrical engineering in 1983, the MSc. degree in mathematics in 1986, and the Ph.D. degree in electrical engineering in 1986, all from the University of Southern California (USC), Los Angeles.

After lecturing for one year at USC, he joined the University of Virginia, Charlottesville, in 1987, where he became a Professor of electrical engineering in 1997. Since 1999, he has been a professor with the Department of Electrical and Computer Engineering, University of Minnesota, Minneapolis, where he now holds an ADC Chair in Wireless Telecommunications. His general interests span the areas of communications and signal processing, estimation and detection theory, time-series analysis, and system identification—subjects on which he has published more than 160 journal papers, 300 conference papers, and two edited books. Current research focuses on transmitter and receiver diversity techniques for single- and multiuser fading communication channels, complex-field and space-time coding, multicarrier, ultrawide band wireless communication systems, cross-layer designs, and distributed sensor networks.

Dr. Giannakis is the (co-) recipient of four best paper awards from the IEEE Signal Processing (SP) Society in 1992, 1998, 2000, and 2001. He also received the Society's Technical Achievement Award in 2000. He served as Editor in Chief for the IEEE SIGNAL PROCESSING LETTERS, as Associate Editor for the IEEE TRANSACTIONS ON SIGNAL PROCESSING and the IEEE SIGNAL PROCESSING LETTERS, as secretary of the SP Conference Board, as member of the SP Publications Board, as member and vice-chair of the Statistical Signal and Array Processing Technical Committee, as chair of the SP for Communications Technical Committee, and as a member of the IEEE Fellows Election Committee. He is currently a member of the the IEEE-SP Society's Board of Governors, the Editorial Board for the PROCEEDINGS OF THE IEEE, and chairs the steering committee of the IEEE TRANSACTIONS ON WIRELESS COMMUNICATIONS.